A von Kármán based nonlinear Kirchhoff plate model coupled with strain gradient elasticity: theory and finite element analysis

Wei Ding, Ziyang Huang, Zongxin Yu, and Adrian Buganza Tepole

School of Mechanical Engineering, Purdue University, West Lafayette, IN 47907

Abstract

In this paper, we explore a von Kármán geometrically nonlinear elastic Kirchhoff plate model with second order strain gradient elasticity theory. To integrate plate theory with nonlinear and strain gradient effects, equations of motion for strain gradient elasticity is first derived started from potential energy representation. Under the assumptions of Kirchhoff plate model, von Kármán strain is then combined with Kirchhoff plate theory to account for geometric nonlinearity. To study the behaviour of this plate theory, a C^0 finite element formulation is developed and a collection of numerical simulations are performed based on the finite element scheme. Numerical experiments show that the proposed methods are able to give numerical solutions to nonlinear strain gradient plate problem and show good convergence characteristics for rectangular spatial discretization.

Keywords— Kirchhoff plate theory, Von-Kárman nonlinearity, Strain gradient elasticity, Finite element method

All correspondence should be addressed to: *abuganza@purdue.edu*

1 Introduction

Classical structural mechanics (SM) theories have been studied started early from several hundred years ago and well established during the development of human society. During the long history, many famous mathematicians and physicians have made great contributions to this subject including, but not limit to, Euler, Bernoulli, Lagrange, and Hamilton [1]. Along with theoretical implementation, these theories have been used in numerous real-world applications and received huge success in multidisciplinary fields such as mechanical, civil [2], and aerospace engineering [3]. Although correctness and effectiveness of classical SM have been testified for a long period, in last century, with the development of modern science, more and more materials with novel physical properties have been discovered that are beyond the capability of original SM theory. Material properties such as hyperelasticity [4], plasticity [5] cannot be captured properly and hence limit SM's potential application. On the other hand, with the existence of computer-aided technology [6] and establishment of continuum mechanics (CM) [7], more and more real-world application opportunities are being substituted by modern methods provided with higher efficiency and accuracy.

Although importance of classical SM is on a downward trend in both science&engineering fields compared with modern methods, many researchers devote to study more advanced SM theories by combining classical theories and novel physical phenomena. In recent decades, many new SM theories have been proposed focusing on micro-scale level problems existing in many areas including porous material [8], composites [9], functionally graded materials (FGM) [10], bio-materials [11], and micro-electromechanical systems (MEMS) [12]. Different from mechanical problem at macro-scale level, it has been discovered experimentally that at micro-scale level, many mechanical structures are endowed with size-dependent properties like non-locality and surface effects [13,14]. These size-dependent properties are often resulted from material heterogeneity: For macro-scale level deformation, effects of material's heterogeneity at micro-scale level on mechanical behaviours are generally

small enough to be ignored; for micro-scale level deformation, material's heterogeneity cannot be ignored when mechanical behaviour is comparable with material length scale. A typical example is that atomic interactions are not negligible when running molecular dynamics simulations [15]. Besides of scale effect, due to some extreme working conditions such as large amplitude vibration, quickly varying external loads, and nonlinear buckling, many micro-structures are often subject to geometrically nonlinear deformation [16]. Motivated by the need of studying material behaviours with size-dependent effect and geometric nonlinearity, many researches have been conducted for micro-structure modeling based on classical SM theories ranging from simple beam theories, to more complicated plate and shell theories.

As one of the most important structure, plate plays a pivotal role in micro-scale structure analysis. Mechanical behaviour of plate with size-dependent properties and geometric nonlinearity has attracted wide interest in both academic and engineering community. Before the study of advanced plate theories, The first plate theory was derived by Kirchhoff and Love [17]. Under the assumption that transverse shear strain is negligible, Kirchhoff-Love plate theory (KLPT) can be seen as an extension of Euler-Bernoulli beam theory. For sufficiently thin plate at macro-scale level, it can be proved that KLPT is able to well predict plate deformation following analytical and experimental validation. To extend classical KLPT's range of application from macro-scale level to micro-scale level, methods have been developed including strain gradient theories (SGT) [18, 19], couple stress theories (CST) [20], and non-local elasticity theories (NET) [21] based on high order strain formulation, micro-structure rotation, and long range interactions, respectively. Among these theories, one of the most famous size-dependent theory called Mindlin's second strain gradient theory (SSGT) [18] was recognized and widely used as advanced elasticity theory. Based on Mindlin's SSGT, a second order negative SGT (NSGT) was proposed by employing second order homogenization technique [22]. In this theory, the constitutive relation is given as

$$\boldsymbol{\sigma} = \mathbf{C}(1 - l^2\nabla^2)\boldsymbol{\varepsilon} \tag{1}$$

where σ, $\mathbf{C}$, l, and $\boldsymbol{\varepsilon}$ are stress, stiffness tensor, material length scale, and strain, respectively. Based on the SGT, size-dependent KLPT has been developed to model micro-scale plate behavior. To further account for nonlinearity, recently a von Kármán based nonlinear strain gradient KLPT (NSGKLPT) was proposed to capture geometrically nonlinear deformation [23]. According to von Kármán nonlinearity, the following Lagrangian Green strain tensor is used in NSGKLPT formulation:

$$\boldsymbol{\varepsilon} = \frac{1}{2}\left(\nabla\boldsymbol{u} + \nabla^T\boldsymbol{u} + \nabla^T\boldsymbol{u}\cdot\nabla\boldsymbol{u}\right) \tag{2}$$

where $\boldsymbol{u}$ is displacement. By combining NSGT and von Kármán nonlinearity, many theoretical results have been presented based on analytic formulation and variational principle [24, 25]. Although these studies have made remarkable progress, analytic solution derivation for NSGKLPT is still an open problem because of the complexity brought by high order derivatives and nonlinearity. Recently, several numerical contributions havs been conducted on developing finite element methods (FEM) [26, 26]. To deal with nonlinearity and strain gradient terms, advanced FEM have been proposed such as isogeometric analysis (IGA) [27] and nonconforming FEM [28]. Many specific applications of these methods have been studied recently: sixth-order boundary value problems are formulated in a variational form within an H^3 Sobolev space setting so that existence and uniqueness of the weak solutions can be established. Discontinuous Galerkin methods (DG) are popular in KL shell and plate problems, involving high-order derivatives, since they provide a means of weakly enforcing the continuity of the unknown-field derivatives. The H^3-conforming isogeometric implementation on NSGKL shell with arbitrary geometry is shown to be able to capture size effects and smoothening stress singularities.

To explore the possibilities of advanced plate theory, in this study we will develop a von Kármán based nonlinear Kirchhoff plate theory coupled with second order strain gradient elasticity and its finite element formulation. This paper is organized as follows: In sec. (2) we show detailed mathematical derivation of NSGKLPT based on the definition of strain gradient potential energy and von Kármán nonlinear strain using varitional principles. Next in sec. (3) we discuss finite element analsis and numerical scheme of our problem including weak form derivation, spatial discretization, and discrete problem formulation. Based on the our

finite element scheme, we show simulation results of parametric studies with respect to nonlinear and strain gradient effects. Algorithm performance analysis is also included in this section. Finally, we end up our study with conclusion.

2 Theoretical formulation of NSGKLPT

In this section we present a detailed mathematical derivation of NSGKLPT by combining Mindlin's SGT and Von Kármán nonlinearity based on classical Kirchhoff's plate theory. Varitional principle is applied for derivation from the perspective of energy method in both SGT and NSGKLPT. We first show how to derive equations of motion for general 3D SGT. Based on Kirchhoff plate assumption and Von Kármán strain definition, we then derive equations of motion for NSGKLPT for homogeneous isotropic plate problem. The final equations of motion for NSGKLPT is represented with nonlinear strain and strain gradient.

2.1 Second order strain gradient elasticity

According to Mindlin's SGT, strain energy density function of homogeneous isotropic material is given as

$$\boldsymbol{U} = \frac{1}{2}\lambda\varepsilon_{ii}\varepsilon_{jj} + \mu\varepsilon_{ij} + c\left(\frac{1}{2}\lambda\varepsilon_{ii,k}\varepsilon_{jj,k} + \mu\varepsilon_{ij,k}\varepsilon_{ij,k}\right) \tag{3}$$

where λ and μ are Lamé parameters and c is material constant which is related with length scale of micro-structure. Consider the following functional

$$\int_t\int_\Omega \boldsymbol{U}d\Omega dt = \int_t\int_\Omega \left(\frac{1}{2}\lambda\varepsilon_{ii}\varepsilon_{jj} + \mu\varepsilon_{ij} + c\left(\frac{1}{2}\lambda\varepsilon_{ii,k}\varepsilon_{jj,k} + \mu\varepsilon_{ij,k}\varepsilon_{ij,k}\right)\right) d\Omega dt \tag{4}$$

and applying variational principle, then the first order variation of above functional can be calculated as

$$\begin{aligned}
\delta\int_t\int_\Omega \boldsymbol{U}d\Omega dt &= \delta\int_t\int_V \left(\frac{1}{2}\lambda\varepsilon_{ii}\varepsilon_{jj} + \mu\varepsilon_{ij}\varepsilon_{ij} + c(\frac{1}{2}\lambda\varepsilon_{ii,k}\varepsilon_{jj,k} + \mu\varepsilon_{ij,k}\varepsilon_{ij,k})\right) d\Omega dt \\
&= \int_t\int_\Omega \left(\lambda\varepsilon_{ii}\delta\varepsilon_{jj} + 2\mu\varepsilon_{ij}\delta\varepsilon_{ij} + c(\lambda\varepsilon_{rr,k}\delta\varepsilon_{jj,k} + 2\mu\varepsilon_{ij,k}\delta\varepsilon_{ij,k})\right) d\Omega dt \\
&= \int_t\int_\Omega \left((2\mu\varepsilon_{ij} + \lambda\varepsilon_{rr}\delta_{ij})\delta\varepsilon_{ij} + c\nabla(2\mu\varepsilon_{ij} + \lambda\varepsilon_{rr}\delta_{ij})\cdot\nabla\delta\varepsilon_{ij}\right) d\Omega dt \\
&= \int_t\int_\Omega (1 - c\nabla^2)(2\mu\varepsilon_{ij} + \lambda\varepsilon_{rr}\delta_{ij})\delta\varepsilon_{ij}d\Omega dt + c\int_t\int_\Gamma \left(\boldsymbol{n}\cdot\nabla(2\mu\varepsilon_{ij} + \lambda\varepsilon_{rr}\delta_{ij})\delta\varepsilon_{ij}\right) d\Gamma dt
\end{aligned} \tag{5}$$

In analogy with classical elasticity theory which defines strain tensor as $\sigma_{ij} = \lambda\delta_{ij}\varepsilon_{kk} + 2\mu\varepsilon_{ij}$, for nonlinear strain gradient theory we define stress tensor as

$$\sigma_{ij} = (1 - c\nabla^2)(\lambda\delta_{ij}\varepsilon_{kk} + 2\mu\varepsilon_{ij}) \tag{6}$$

Applying divergence theorem as follows

$$\int_t\int_\Omega \sigma_{ij}\delta\varepsilon_{ij}d\Omega dt = \int_t\int_\Gamma \boldsymbol{n}\cdot\sigma_{ij}\delta u_i d\Gamma dt - \int_t\int_\Omega \nabla\cdot\sigma_{ij}\delta u_i d\Omega dt \tag{7}$$

and substituting stress back into Eqn.(), we obtain that

$$\begin{aligned}
\delta\int_t\int_\Omega \boldsymbol{U}d\Omega dt &= -\int_t\int_\Omega \nabla\cdot\sigma_{ij}\delta u_i d\Omega dt + B.O.U.N \\
B.O.U.N &= \int_t\int_\Gamma \left(\boldsymbol{n}\cdot\sigma_{ij}\delta u_i + c\boldsymbol{n}\cdot\nabla(2\mu\varepsilon_{ij} + \lambda\varepsilon_{rr}\delta_{ij})\delta\varepsilon_{ij}\right) d\Gamma dt
\end{aligned} \tag{8}$$

here $B.O.U.N$ indicates boundary terms. Moreover, considering variation of kinetic energy and work done by external forces and employing Hamilton's principle,

$$\delta \int_t (\mathcal{T} - \mathcal{U} + \mathcal{W}) dt = \int_t \int_\Omega (-\rho \ddot{\boldsymbol{u}} + \nabla \cdot \boldsymbol{\sigma} + \rho \boldsymbol{f}) \delta \boldsymbol{u} d\Omega dt + B.O.U.N = 0 \tag{9}$$

We obtain equations of motion for Mindlin's first SGT as

$$\rho \ddot{\boldsymbol{u}} = \nabla \cdot \boldsymbol{\sigma} + \rho \boldsymbol{f} \tag{10}$$

2.2 Equations of motion for NSGKLPT

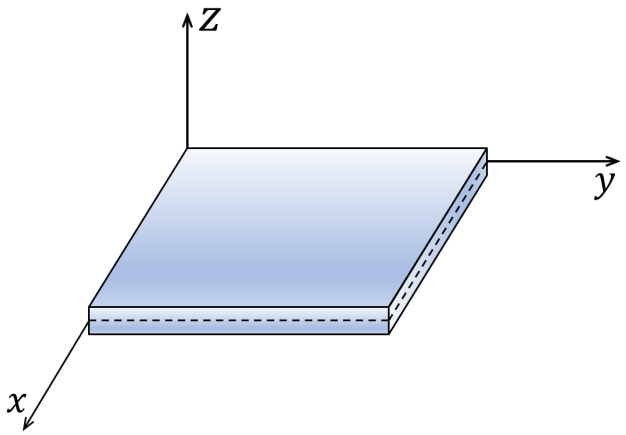

Figure 1: Schematic illustration of Kirchhoff plate.

According to Kirchhoff plate theory, displacement field $\boldsymbol{u} = [u, v, w]^T$ at point (x, y, z) over the whole plate can be expressed using corresponding mid-plane displacement field $\hat{\boldsymbol{u}} = [\hat{u}, \hat{v}, \hat{w}]^T$ at point $(x, y, 0)$. Their relations between two displacement field are given as

$$\begin{aligned} u(x, y, z) &= \hat{u}(x, y) - z \frac{\partial \hat{w}}{\partial x} \\ v(x, y, z) &= \hat{v}(x, y) - z \frac{\partial \hat{w}}{\partial y} \\ w(x, y, z) &= \hat{w}(x, y) \end{aligned} \tag{11}$$

where $w = \hat{w}$ is out-of-plane displacement which is not dependent on z. Based on Eqn.(2), Normal components of Lagrange Green strain tensor then can be written as

$$\begin{aligned} \varepsilon_{xx} &= \frac{\partial \hat{u}}{\partial x} - z \frac{\partial^2 \hat{w}}{\partial x^2} + \frac{d}{2} \left(z^2 \left(\frac{\partial^2 \hat{w}}{\partial x^2} \right)^2 + z^2 \left(\frac{\partial^2 \hat{w}}{\partial x \partial y} \right)^2 + \left(\frac{\partial \hat{w}}{\partial x} \right)^2 \right) \\ \varepsilon_{yy} &= \frac{\partial \hat{u}}{\partial y} - z \frac{\partial^2 \hat{w}}{\partial y^2} + \frac{d}{2} \left(z^2 \left(\frac{\partial^2 \hat{w}}{\partial y^2} \right)^2 + z^2 \left(\frac{\partial^2 \hat{w}}{\partial x \partial y} \right)^2 + \left(\frac{\partial \hat{w}}{\partial y} \right)^2 \right) \\ \varepsilon_{zz} &= \frac{d}{2} \left(\left(\frac{\partial \hat{w}}{\partial x} \right)^2 + \left(\frac{\partial \hat{w}}{\partial y} \right)^2 \right) \end{aligned} \tag{12}$$

and shear components are given as

$$\begin{aligned}
\varepsilon_{xy} &= \frac{1}{2}\frac{\partial \hat{u}}{\partial y} + \frac{1}{2}\frac{\partial \hat{v}}{\partial x} - z\frac{\partial^2 \hat{w}}{\partial x \partial y} + \frac{d}{2}\left(z^2 \frac{\partial^2 \hat{w}}{\partial x^2}\frac{\partial^2 \hat{w}}{\partial x \partial y} + z^2 \frac{\partial^2 \hat{w}}{\partial y^2}\frac{\partial^2 \hat{w}}{\partial x \partial y} + \frac{\partial \hat{w}}{\partial x}\frac{\partial \hat{w}}{\partial y}\right) \\
\varepsilon_{xz} &= \frac{d}{2}\left(z\frac{\partial \hat{w}}{\partial y}\frac{\partial^2 \hat{w}}{\partial x \partial y} + z\frac{\partial \hat{w}}{\partial x}\frac{\partial^2 \hat{w}}{\partial x^2}\right) \\
\varepsilon_{yz} &= \frac{d}{2}\left(z\frac{\partial \hat{w}}{\partial x}\frac{\partial^2 \hat{w}}{\partial x \partial y} + z\frac{\partial \hat{w}}{\partial y}\frac{\partial^2 \hat{w}}{\partial y^2}\right)
\end{aligned} \tag{13}$$

In this study we use an extra factor d ranging from 0 to 1 to control the ratio of Von Kármán nonlineartity. It can be seen that Lagrange Green strain tensor contains both nonlinear and high order terms. To obtain von Kármán nonlinear strain-displacement relations, small strains and moderate rotations conditions are considered such that nonlinear and high order terms can be neglected except for $\left\{\left(\frac{\partial \hat{w}}{\partial x}\right)^2, \left(\frac{\partial \hat{w}}{\partial y}\right)^2, \frac{\partial \hat{w}}{\partial x}\frac{\partial \hat{w}}{\partial y}\right\}$. By employing this condition, von Kármán strain-displacement relation can be derived as

$$\begin{aligned}
\varepsilon_{xx} &= \frac{\partial \hat{u}}{\partial x} - z\frac{\partial^2 \hat{w}}{\partial x^2} + \frac{d}{2}\left(\frac{\partial \hat{w}}{\partial x}\right)^2 \\
\varepsilon_{yy} &= \frac{\partial \hat{v}}{\partial y} - z\frac{\partial^2 \hat{w}}{\partial y^2} + \frac{d}{2}\left(\frac{\partial \hat{w}}{\partial y}\right)^2 \\
\varepsilon_{xy} &= \frac{1}{2}\frac{\partial \hat{u}}{\partial y} + \frac{1}{2}\frac{\partial \hat{v}}{\partial x} - z\frac{\partial^2 \hat{w}}{\partial x \partial y} + \frac{d}{2}\frac{\partial \hat{w}}{\partial x}\frac{\partial \hat{w}}{\partial y} \\
\varepsilon_{zz} &= \varepsilon_{xz} = \varepsilon_{yz} = 0
\end{aligned} \tag{14}$$

where the first three components are in-plane von Kármán strain and remaining three components are out-of-plane von Kármán strain which equal zero under Kirchhoff plate assumption. Based on this condition, in the remaining part of this paper we only consider in-plane cases for vector and tensor calculation. To simplify symbolic expressions, we denote von Kármán strain as

$$\begin{aligned}
\boldsymbol{\varepsilon} &= \frac{1}{2}\left(\nabla \hat{\boldsymbol{u}} + \nabla^T \hat{\boldsymbol{u}} - 2z\nabla(\nabla w) + d\nabla w \otimes \nabla w\right) \\
&= \frac{1}{2}\left(\nabla \hat{\boldsymbol{u}} + \nabla^T \hat{\boldsymbol{u}} + d\nabla w \otimes \nabla w\right) - z\nabla(\nabla w) \\
&= \boldsymbol{\epsilon} - z\boldsymbol{\chi}
\end{aligned} \tag{15}$$

where $\otimes$ denotes outer product. $\boldsymbol{\epsilon} = \frac{1}{2}\left(\nabla \hat{\boldsymbol{u}} + \nabla^T \hat{\boldsymbol{u}} + d\nabla w \otimes \nabla w\right)$ and $\boldsymbol{\chi} = \nabla(\nabla w)$ are two portions of von Kármán strain which are called z-relevant strain and z-irrelevant strain in this paper. We will use these definition later on to simplify finite element formulation. Having von Kármán strain representation, we now extend classical KLPT to NSGKLPT by incorporating SGT we have derived in previous section. Similar with the derivation of SGT, we also use variational principle to derive equations of motion for NSGKLPT. Consider first order variation of following functional

$$\int_t \int_\Omega \boldsymbol{\sigma} : \boldsymbol{\varepsilon} d\Omega dt = \int_t \int_\Gamma \int_{-\frac{h}{2}}^{\frac{h}{2}} (1 - c\nabla^2) C_{ijkl}\varepsilon_{kl}\varepsilon_{ij} dz d\Gamma dt \tag{16}$$

which is total strain potential energy for the whole plate. Based on the fact that Laplace operator is self-adjoint

and stiffness tensor C_{ijkl} is symmetric, we apply variational principle and obtain that

$$\begin{aligned}
\frac{1}{2}\delta\int_t\int_\Omega \boldsymbol{\sigma}:\boldsymbol{\varepsilon}d\Omega dt &= \int_t\int_\Gamma\int_{-\frac{h}{2}}^{\frac{h}{2}}\frac{1}{2}\left(\delta(1-c\nabla^2)\left(C_{ijkl}\varepsilon_{kl}\right)\varepsilon_{ij}+(1-c\nabla^2)C_{ijkl}\varepsilon_{kl}\delta\varepsilon_{ij}\right)dzd\Gamma dt \\
&= \frac{1}{2}\int_t\int_\Gamma\int_{-\frac{h}{2}}^{\frac{h}{2}}C_{ijkl}\left(\delta(1-c\nabla^2)\varepsilon_{ij}\varepsilon_{kl}+(1-c\nabla^2)\varepsilon_{kl}\delta\varepsilon_{ij}\right)dzd\Gamma dt \\
&= \int_t\int_\Gamma\int_{-\frac{h}{2}}^{\frac{h}{2}}\left(1-c\nabla^2\right)\left(C_{ijkl}\varepsilon_{kl}\right)\delta\varepsilon_{ij}dzd\Gamma dt \\
&= \int_t\int_\Gamma\int_{-\frac{h}{2}}^{\frac{h}{2}}\boldsymbol{\sigma}:\delta\boldsymbol{\varepsilon}dzd\Gamma dt
\end{aligned} \tag{17}$$

To obtain equations of motion of NSGKLPT with the form of stress resultants, we substitute von Kármán strain into above equation and further simplify it as

$$\begin{aligned}
\int_t\int_\Gamma\int_{-\frac{h}{2}}^{\frac{h}{2}}\boldsymbol{\sigma}:\delta\boldsymbol{\varepsilon}dzd\Gamma dt &= \frac{1}{2}\int_t\int_\Gamma\int_{-\frac{h}{2}}^{\frac{h}{2}}\sigma_{ij}\delta\left(u_{i,j}+u_{j,i}+dw_{,i}w_{,j}-2zw_{,ij}\right)dzd\Gamma dt \\
&= \frac{1}{2}\int_t\int_\Gamma\left(N_{ij}\delta u_{i,j}+N_{ij}\delta u_{j,i}+dN_{ij}\delta(w_{,i}w_{,j})-2M_{ij}\delta w_{,ij}\right)d\Gamma dt \\
&= \frac{1}{2}\int_t\int_\Gamma-\left(N_{ij,j}\delta u_i+N_{ij,i}\delta u_j+(d(N_{ij}w_{,j})_{,i}+d(N_{ij}w_{,i})_{,j}+2M_{ij,ij})\delta w\right)d\Gamma dt \\
&+ \frac{1}{2}\int_t\int_{\partial\Gamma}\left(\boldsymbol{n}\cdot N_{ij}\delta u_i+\boldsymbol{n}\cdot N_{ij}\delta u_j\right)dLdt \\
&+ \frac{1}{2}\int_t\int_{\partial\Gamma}\boldsymbol{n}\cdot\left(dN_{ij}w_{,j}+dN_{ij}w_{,i}+2M_{ij,j}\right)\delta w dLdt \\
&- \int_t\int_{\partial\Gamma}\boldsymbol{n}\cdot M_{ij}\delta w_{,i}dLdt
\end{aligned} \tag{18}$$

Considering kinetic energy and work done by external loading we have derived previously in Sec. (), equations of motion for NSGKLPT can now be obtained as

$$\begin{aligned}
N_{ij,j} &= \rho\ddot{u}_i \\
d(N_{ij}w_{,j})_{,i}+M_{ij,ij}-f &= \rho\ddot{w}
\end{aligned} \tag{19}$$

and boundary conditions

$$\begin{aligned}
n_jN_{ij} &= T_i^1 \quad \text{or} \quad \delta u_i=0 \quad \text{at} \quad \partial\Gamma \\
n_j\left(N_{ij}w_{,i}+M_{ij,i}\right) &= T^2 \quad \text{or} \quad \delta w=0 \quad \text{at} \quad \partial\Gamma \\
n_jM_{ij} &= T_i^3 \quad \text{or} \quad \delta w_{,i}=0 \quad \text{at} \quad \partial\Gamma
\end{aligned} \tag{20}$$

where

$$\begin{aligned}
N_{ij} &= \int_{-\frac{h}{2}}^{\frac{h}{2}}\sigma_{ij}dz = h(1-c\nabla^2)C_{ijkl}\epsilon_{kl} \\
M_{ij} &= \int_{-\frac{h}{2}}^{\frac{h}{2}}\sigma_{ij}zdz = -\frac{h^3}{12}(1-c\nabla^2)C_{ijkl}\chi_{kl}
\end{aligned} \tag{21}$$

are nonlinear stress and moment resultants, respectively (integrals are evaluated by assuming isotropic homogeneous material). T^1, T^2, and T^3 refer general traction applied for three boundary conditions.

3 Finite element analysis

We try to find solutions u in Sobolev space with compact support $V = H_0^1(\Gamma) := \{v \in L^2(\Gamma) | \nabla v \in L^2(\Gamma), v|_{\partial\Gamma} = 0\}$ for our high order PDE problem. Generally speaking, numerical solutions for high order problems require approximations with high order continuity. In FEM this condition can be satisfied usually by using high order shape functions such as Hermite polynomials and B-spline function. Instead of using high order shape functions, in this study we will introduce extra variables and equations to lower down order of original PDE problem such that linear shape function is used to give approximate solution for each equation.

3.1 Derivation of weak form, residual, and tangent

In this study we only consider static response of NSGKLPT. In order to eliminate high order derivatives (more than 2^{nd} order) evaluation during weak form formulation, intermediate variables and equations are required to be introduced. We decide to use following equations to state the problem:

$$\begin{aligned}
\theta_{ij,j} - c(C_{ijkl}\vartheta_{kl})_{,j} &= 0 \\
d((\theta_{ij} - c\vartheta_{ij})w_{,j})_{,i} + (\phi_{ij} - cC_{ijkl}\varphi_{kl})_{,ij} &= -\frac{12}{h^3}f \\
\theta_{ij} &= C_{ijkl}\epsilon_{kl} = (A\epsilon_{ij} + B\delta_{ij}\epsilon_{kk}) \\
\vartheta_{ij} &= \nabla^2\epsilon_{kl} \\
\phi_{ij} &= C_{ijkl}\chi_{kl} = (A\chi_{ij} + B\delta_{ij}\chi_{kk}) \\
\varphi_{ij} &= \nabla^2\chi_{kl} \\
\epsilon_{ij} &= \frac{1}{2}(\hat{u}_{i,j} + \hat{u}_{j,i} + dw_{,i}w_{,j}) \\
\chi_{ij} &= w_{,ij}
\end{aligned} \tag{22}$$

Under plane stress assumption for isotropic homogeneous material, material constants are given as $A = \frac{E(1-\nu)}{1-\nu^2}$ and $B = \frac{E\nu}{1-\nu^2}$ where E and ν are Young's modulus and Poisson ratio, respectively. Noticing that the highest order derivative of w is up to 6^{th} order, which is difficult to deal with using basic FEM techniques. To simplify FEM formulation, in the following work we will ignore 6^{th} order derivative term. Based on this assumption, we consider following 12 unknown variables fields as

$$\boldsymbol{U} = [w, \hat{u}_{ij}, \epsilon_{ij}, \vartheta_{ij}, \chi_{ij}] = [w, \hat{\boldsymbol{u}}, \boldsymbol{\epsilon}, \boldsymbol{\vartheta}, \boldsymbol{\chi}] \tag{23}$$

and further simplify Eqn. (23), we have the following sets of nonlinear partial differential equation (PDE)

$$\begin{aligned}
0 &= d\nabla\cdot(\boldsymbol{C}:\boldsymbol{\epsilon}\cdot\nabla w + \nabla\cdot(\boldsymbol{C}:\boldsymbol{\chi})) + \frac{12}{h^3}f \\
0 &= \nabla\cdot\left(\boldsymbol{C}:\frac{1}{2}\left(\nabla\hat{\boldsymbol{u}} + \nabla^T\hat{\boldsymbol{u}} + d\nabla w\otimes\nabla w\right) - c\boldsymbol{C}:\boldsymbol{\vartheta}\right) \\
\boldsymbol{\epsilon} &= \frac{1}{2}\left(\nabla\hat{\boldsymbol{u}} + \nabla^T\hat{\boldsymbol{u}} + d\nabla w\otimes\nabla w\right) \\
\boldsymbol{\vartheta} &= \nabla^2\boldsymbol{\epsilon} \\
\boldsymbol{\chi} &= \nabla(\nabla w)
\end{aligned} \tag{24}$$

with total 12 independent equations and 12 variables. Although the problem formulation is fairly complicated, provided that in each equation the highest order of derivative is no more than 2, theoretically this problem can be solved without introducing high order FEM. Using divergence theorem, the weak form of Eqn. (24)

can now be immediately derived as

$$
\begin{aligned}
0 &= \int_{\partial\Gamma} (\boldsymbol{C} : \boldsymbol{\epsilon} \cdot \nabla w + \nabla \cdot (\boldsymbol{C} : \boldsymbol{\chi})) \cdot \boldsymbol{n} \delta\boldsymbol{\omega}_{\boldsymbol{1}}^{\boldsymbol{S}} dL - \int_{\Gamma} (\boldsymbol{C} : \boldsymbol{\epsilon} \cdot \nabla w + \nabla \cdot (\boldsymbol{C} : \boldsymbol{\chi})) \cdot \nabla \delta\boldsymbol{\omega}_{\boldsymbol{1}}^{\boldsymbol{S}} d\Gamma + \int_{\Gamma} \frac{12}{h^3} f \delta\boldsymbol{\omega}_{\boldsymbol{2}}^{\boldsymbol{S}} d\Gamma \\
0 &= \int_{\partial\Gamma} (\boldsymbol{C} : \boldsymbol{\epsilon} - c\boldsymbol{C} : \boldsymbol{\vartheta}) \cdot \boldsymbol{n} \cdot \delta\boldsymbol{\omega}_{\boldsymbol{2}}^{\boldsymbol{V}} dL - \int_{\Gamma} (\boldsymbol{C} : \boldsymbol{\epsilon} - c\boldsymbol{C} : \boldsymbol{\vartheta}) : \nabla \delta\boldsymbol{\omega}_{\boldsymbol{2}}^{\boldsymbol{V}} d\Gamma \\
0 &= \int_{\Gamma} \left(\nabla \hat{\boldsymbol{u}} + \nabla^T \hat{\boldsymbol{u}} + \nabla w \otimes \nabla w - 2\boldsymbol{\epsilon} \right) : \delta\boldsymbol{\omega}_{\boldsymbol{3}}^{\boldsymbol{M}} d\Gamma \\
0 &= \int_{\partial\Gamma} (\nabla \boldsymbol{\epsilon} \cdot \boldsymbol{n}) : \delta\boldsymbol{\omega}_{\boldsymbol{4}}^{\boldsymbol{M}} dL - \int_{\Gamma} \left(\nabla \boldsymbol{\epsilon} \vdots \nabla \delta\boldsymbol{\omega}_{\boldsymbol{3}}^{\boldsymbol{M}} + \boldsymbol{\vartheta} : \delta\boldsymbol{\omega}_{\boldsymbol{4}}^{\boldsymbol{M}} \right) d\Gamma \\
0 &= \int_{\partial\Gamma} (\boldsymbol{n} \otimes \nabla w) : \delta\boldsymbol{\omega}_{\boldsymbol{5}}^{\boldsymbol{M}} dL - \int_{\Gamma} \left(\nabla w \cdot (\nabla \cdot \delta\boldsymbol{\omega}_{\boldsymbol{5}}^{\boldsymbol{M}}) + \boldsymbol{\chi} : \delta\boldsymbol{\omega}_{\boldsymbol{5}}^{\boldsymbol{M}} \right) d\Gamma
\end{aligned}
\tag{25}
$$

where $\delta\boldsymbol{\omega} = \left[\delta\boldsymbol{\omega}_{\boldsymbol{1}}^{\boldsymbol{V}}, \delta\boldsymbol{\omega}_{\boldsymbol{2}}^{\boldsymbol{S}}, \delta\boldsymbol{\omega}_{\boldsymbol{3}}^{\boldsymbol{M}}, \delta\boldsymbol{\omega}_{\boldsymbol{4}}^{\boldsymbol{M}}, \delta\boldsymbol{\omega}_{\boldsymbol{5}}^{\boldsymbol{M}}\right]$ are virtual variables. Superscript $\boldsymbol{S}$, $\boldsymbol{V}$, and $\boldsymbol{M}$ over variables indicate that these variables are scalars, vectors, and matrices, respectively. For homogeneous boundary condition, we consider a finite dimensional subspace $V_h \subset V$ such that $V_h = \text{span}\{\delta\boldsymbol{\omega}_{\boldsymbol{1}}^{\boldsymbol{V}}, \delta\boldsymbol{\omega}_{\boldsymbol{2}}^{\boldsymbol{S}}, \delta\boldsymbol{\omega}_{\boldsymbol{3}}^{\boldsymbol{M}}, \delta\boldsymbol{\omega}_{\boldsymbol{4}}^{\boldsymbol{M}}, \delta\boldsymbol{\omega}_{\boldsymbol{5}}^{\boldsymbol{M}}\}$. Applying method of weighted residuals, residuals of weak form can be easily given as

$$
\begin{aligned}
\boldsymbol{R}_{\boldsymbol{1}}^{\boldsymbol{S}} &= \int_{\Gamma} (\boldsymbol{C} : \boldsymbol{\epsilon} \cdot \nabla w + \nabla \cdot (\boldsymbol{C} : \boldsymbol{\chi})) \cdot \nabla \delta\boldsymbol{\omega}_{\boldsymbol{1}}^{\boldsymbol{S}} d\Gamma - \int_{\Gamma} \frac{12}{h^3} f \delta\boldsymbol{\omega}_{\boldsymbol{1}}^{\boldsymbol{S}} d\Gamma \\
\boldsymbol{R}_{\boldsymbol{2}}^{\boldsymbol{V}} &= \int_{\Gamma} (\boldsymbol{C} : \boldsymbol{\epsilon} - c\boldsymbol{C} : \boldsymbol{\vartheta}) : \nabla \delta\boldsymbol{\omega}_{\boldsymbol{2}}^{\boldsymbol{V}} d\Gamma \\
\boldsymbol{R}_{\boldsymbol{3}}^{\boldsymbol{M}} &= \int_{\Gamma} \left(\nabla \hat{\boldsymbol{u}} + \nabla^T \hat{\boldsymbol{u}} + \nabla w \otimes \nabla w - 2\boldsymbol{\epsilon} \right) : \delta\boldsymbol{\omega}_{\boldsymbol{3}}^{\boldsymbol{M}} d\Gamma \\
\boldsymbol{R}_{\boldsymbol{4}}^{\boldsymbol{M}} &= \int_{\Gamma} \left(\nabla \boldsymbol{\epsilon} \vdots \nabla \delta\boldsymbol{\omega}_{\boldsymbol{4}}^{\boldsymbol{M}} + \boldsymbol{\vartheta} : \delta\boldsymbol{\omega}_{\boldsymbol{4}}^{\boldsymbol{M}} \right) d\Gamma \\
\boldsymbol{R}_{\boldsymbol{5}}^{\boldsymbol{M}} &= \int_{\Gamma} \left(\nabla w \cdot (\nabla \cdot \delta\boldsymbol{\omega}_{\boldsymbol{5}}^{\boldsymbol{M}}) + \boldsymbol{\chi} : \delta\boldsymbol{\omega}_{\boldsymbol{5}}^{\boldsymbol{M}} \right) d\Gamma
\end{aligned}
\tag{26}
$$

and tangent

$$
\begin{aligned}
\Delta\boldsymbol{R}_{\boldsymbol{1}}^{\boldsymbol{S}} &= \int_{\Gamma} (\boldsymbol{C} : \Delta\boldsymbol{\epsilon} \cdot \nabla w + \boldsymbol{C} : \boldsymbol{\epsilon} \cdot \nabla(\Delta w) + \nabla \cdot (\boldsymbol{C} : \Delta\boldsymbol{\chi})) \cdot \nabla \delta\boldsymbol{\omega}_{\boldsymbol{1}}^{\boldsymbol{S}} d\Gamma \\
\Delta\boldsymbol{R}_{\boldsymbol{2}}^{\boldsymbol{V}} &= \int_{\Gamma} (\boldsymbol{C} : \Delta\boldsymbol{\epsilon} - c\boldsymbol{C} : \Delta\boldsymbol{\vartheta}) : \nabla \delta\boldsymbol{\omega}_{\boldsymbol{2}}^{\boldsymbol{V}} d\Gamma \\
\Delta\boldsymbol{R}_{\boldsymbol{3}}^{\boldsymbol{M}} &= \int_{\Gamma} \left(\nabla(\Delta\hat{\boldsymbol{u}}) + \nabla^T(\Delta\hat{\boldsymbol{u}}) + \nabla(\Delta w) \otimes \nabla w + \nabla w \otimes \nabla(\Delta w) - 2\Delta\boldsymbol{\epsilon} \right) : \delta\boldsymbol{\omega}_{\boldsymbol{3}}^{\boldsymbol{M}} d\Gamma \\
\Delta\boldsymbol{R}_{\boldsymbol{4}}^{\boldsymbol{M}} &= \int_{\Gamma} \left(\nabla(\Delta\boldsymbol{\epsilon}) \vdots \nabla \delta\boldsymbol{\omega}_{\boldsymbol{4}}^{\boldsymbol{M}} + \Delta\boldsymbol{\vartheta} : \delta\boldsymbol{\omega}_{\boldsymbol{4}}^{\boldsymbol{M}} \right) d\Gamma \\
\Delta\boldsymbol{R}_{\boldsymbol{5}}^{\boldsymbol{M}} &= \int_{\Gamma} \left(\nabla(\Delta w) \cdot (\nabla \cdot \delta\boldsymbol{\omega}_{\boldsymbol{5}}^{\boldsymbol{M}}) + \Delta\boldsymbol{\chi} : \delta\boldsymbol{\omega}_{\boldsymbol{5}}^{\boldsymbol{M}} \right) d\Gamma
\end{aligned}
\tag{27}
$$

It should be mentioned that even if we have ignored 6^{th} order derivative term, the weak form, residual, and tangent formulations still affected by strain gradient effect through variable $\boldsymbol{\vartheta} = \nabla^2\boldsymbol{\epsilon}$ and nonlinear effect through variable $\boldsymbol{\chi} = \nabla(\nabla w)$. Based on above formulations, in next section we will show how to perform discretization and finite element approximation.

3.2 Spatial discretization and finite element formulation

For static deformation case, we only consider spatial discretization. As shown Fig. (2), in this study, we use 4-node quadrilateral element to perform finite element dicretization. Based on weak form derivation in Sec.

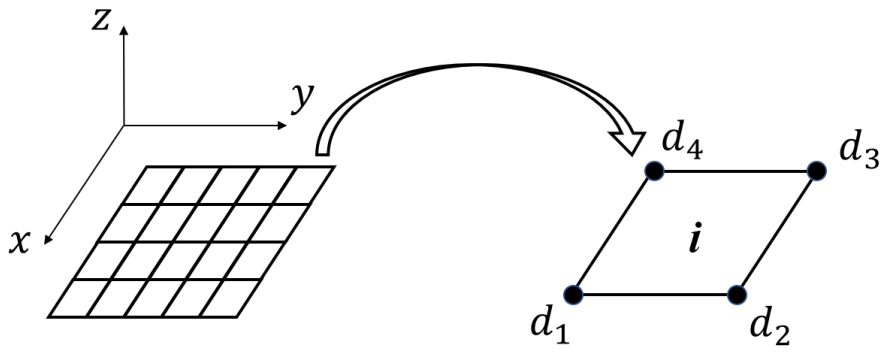

Figure 2: Geometry discretization. Rectangular plate in 2D $x-y$ plane is discretized by quadrilateral elements. For each element shown in above figure, we define nodal degrees of freedom $\boldsymbol{d}_i$ at each nodal point $i = 1, 2, 3, 4$. For each $\boldsymbol{d}_i$, it contains 12 degrees of freedom defined by previous unknown variables $[w, \hat{\boldsymbol{u}}, \boldsymbol{\epsilon}, \boldsymbol{\vartheta}, \boldsymbol{\chi}]$. Total 48 degrees of freedom is contained for one element.

(3.1), at each node inside one element, we consider nodal degrees of freedom $\boldsymbol{d}_i$ given as

$$\boldsymbol{d}_i = \{w, \hat{u}_x, \hat{u}_y, \epsilon_{xx}, \epsilon_{yy}, \epsilon_{xy}, \vartheta_{xx}, \vartheta_{yy}, \vartheta_{xy}, \chi_{xx}, \chi_{yy}, \chi_{xy}\}_i^T, \quad i = 1, 2, 3, 4 \tag{28}$$

For original plate deformation problem, theoretically at each node only 3 displacement variables $\{w, \hat{u}_x, \hat{u}_y\}$ need to be solved as degrees of freedom. But this strategy requires not only full expansion of Eqn. (19) using $\{w, \hat{u}_x, \hat{u}_y\}$ for weak form derivation, but also the use of high order interpolation to guarantee continuity. Under the governance of Von Kármán nonlinearity and strain gradient elasticity, finite element analysis would becomes much more complicated (see [26]). To avoid the inconvenience, in this study we decide to add degrees of freedom at each node. Based on the configuration of degrees of freedom, linear shape functions are adopted for approximation.

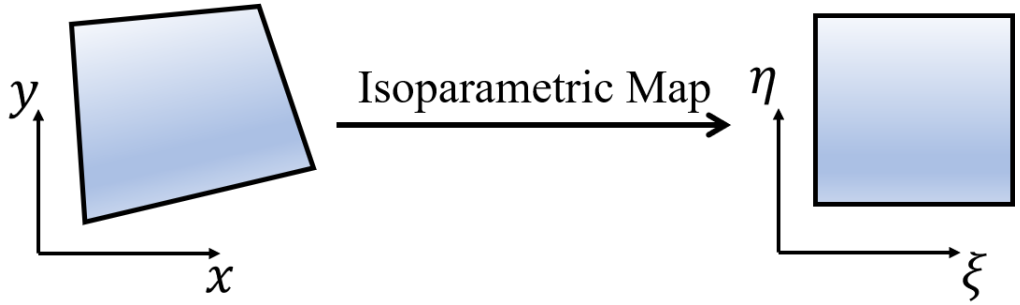

Figure 3: Isoparametric map from physical element domain (x, y) to parent domain (ξ, η). Linear shape functions is defined in parent domain.

As shown in fig. (3), here we define linear shape functions in parent domain and transform from physical domain to parent domain by isoparametric map. In parent domain, shape functions at each nodal point are given as

$$N_\alpha(\xi, \eta) = \frac{1}{4}(1 + \xi_\alpha \xi)(1 + \eta_\alpha \eta), \quad \alpha = 1, 2, 3, 4 \tag{29}$$

where values of ξ_α and η_I can be chosen as -1 or 1 for different nodal point. To discretize residual and

tangent, inside each element e, virtual variables $\delta\boldsymbol{\omega}$, $\delta\boldsymbol{\omega^V}$, and $\delta\boldsymbol{\omega^M}$ with different dimensions are chosen as

$$\begin{aligned}
\delta\omega^S &= N_\alpha(\xi,\eta) \\
\delta\omega^V &= [N_\alpha(\xi,\eta),0]^T, \quad [0,N_\alpha(\xi,\eta)]^T \\
\delta\omega^M &= \begin{bmatrix} N_\alpha(\xi,\eta) & 0 \\ 0 & 0 \end{bmatrix}, \quad \begin{bmatrix} 0 & N_\alpha(\xi,\eta) \\ N_\alpha(\xi,\eta) & 0 \end{bmatrix}, \quad \begin{bmatrix} 0 & 0 \\ 0 & N_\alpha(\xi,\eta) \end{bmatrix}, \\
\alpha &= 1,2,3,4.
\end{aligned}$$

and scalar unknown $\hat{U}$ is approximated by linear interpolation

$$\hat{U} = \sum_{\beta=1}^{4} \hat{U}_\beta^e N_\beta(\xi,\eta). \tag{30}$$

With such a setup, one can easily compute the residuals in Eq.(26). For example

$$R_1^e = \boldsymbol{R_1^{S,1}} = \int_\Gamma (\boldsymbol{C}:\boldsymbol{\epsilon}\cdot\nabla w + \nabla\cdot(\boldsymbol{C}:\boldsymbol{\chi}))\cdot\nabla N_1 d\Gamma - \int_\Gamma \frac{12}{h^3} f N_1 d\Gamma, \tag{31}$$

where R_1^e is the first row of the elemental residual.

To obtain the stiffness matrix, we need to obtain the partial derivative of the residuals with respect to the degree of freedoms. For a clear presentation, we provide the following example. We consider tangent ΔR_1^S and obtain $\partial R_1^S/\partial w^e$ from it in element e. First, all the degree of freedoms in the element are zero except Δw_β^e. As a result from Eq.(26), we obtain

$$\Delta\boldsymbol{R_1^{S,\alpha}} = \int_\Gamma (\boldsymbol{C}:\boldsymbol{\epsilon}\cdot\nabla(\Delta w))\cdot\nabla N_\alpha d\Gamma. \tag{32}$$

As already known that $w = \sum_{\gamma=1}^4 w_\gamma^e N_\gamma = w_\beta^e N_\beta$, we have

$$\Delta\boldsymbol{R_1^{S,\alpha}} = \Delta w_\beta^e \int_\Gamma (\boldsymbol{C}:\boldsymbol{\epsilon}\cdot\nabla N_\beta)\cdot\nabla N_\alpha d\Gamma. \tag{33}$$

Finally, the partial derivative can be calculated by

$$\frac{\partial R_1^{S,\alpha}}{\partial w_\beta^e} = \frac{\Delta\boldsymbol{R_1^{S,\alpha}}}{\Delta w_\beta^e} = \int_\Gamma (\boldsymbol{C}:\boldsymbol{\epsilon}\cdot\nabla N_\beta)\cdot\nabla N_\alpha d\Gamma, \tag{34}$$

which is one of the components of the elemental stiffness matrix, and any other components in the elemental stiffness matrix are determined in the same manner. As for numerical integration, all above integrals in this study are computed with 4 point Gaussian quadrature rule, such that

$$\int_{-1}^{1} f(\xi) d\xi = \sum_{ip=1}^{4} \omega_{G,ip} f(\xi_{G,ip}), \tag{35}$$

where ω_G and ξ_G are Gaussian quadrature weights and points, respectively. By incorporating above procedure, for $n\times n$ spatial discretization, eventually we will get a fully discretized tangent matrix with shape $12n\times 12n$ which can be solved using Newton-Raphson iteration method. In next section we will show numerical simulation results based on our finite element scheme.

4 Numerical simulation

In this section we present a series of numerical simulations with respect to NSGKLPT using the proposed FEM. Here we consider a homogeneous isotropic micro-plate bending problem as shown in Fig. (1) with length $L_x = L_y = 1$mm and height $h = 0.1$mm. With all homogeneous boundary conditions (see boundary condition treatment in Sec. (3.1)) on left, right, bottom, and top boundaries, a uniformly distributed transverse loading $f = 1000\text{N/mm}^2$ is added. Material is considered as Aluminum with Young's modulus $E = 6.91\times10^{10}$GPa and Poisson's ratio $\nu = 0.33$.

4.1 Parametric studies of nonlinear and strain gradient effect

Fig. (4) shows 15×15 mesh and corresponding out-of-plane displacement. It is seen that under uniformly distributed transverse loading, the radially distributed simulation result shows good consistence with classical plate testing results. The maximum displacement is much larger compared with size of micro plate, which is might because of we ignore all boundary condition terms in finite element formulation. Different from classical FEM, in this study we introduced extra 9 equations and hence with extra 9 boundary integrals in weak form formulation derived by divergence theorem. Unlike classical plate deformation problems whose 3 boundary integrals have explicit physical meanings such as free boundary, clamped boundary, and simply supported boundary conditions, in this problem the boundary integral are highly coupled with nonlinear and strain gradient terms which make even harder to interpret the connection between those 9 extra boundary integrals and physical meaningful boundary conditions.

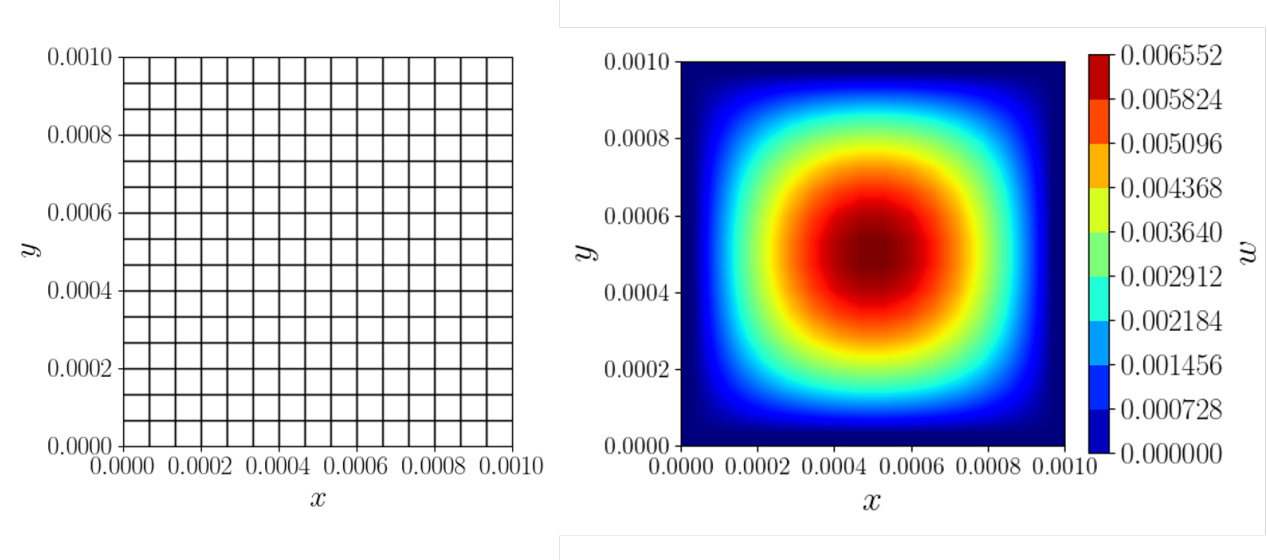

Figure 4: The mesh (left) and the out-of-plane deformation contour (right).

Fig. (5) shows parametric study results in terms of nonlinear and strain gradient effects based on the same configuration. From (a) it can be observed that with the increase of nonlinear effect, the overall displacement becomes larger and larger. This trend is consistent with theory assumption simply because the existence of nonlinearity allows our model to capture larger strain than classical linear Kirchhoff plate model. For the effect of strain gradient, a decreasing trend can be observed when characteristic length factor c increases. This results is also as it is expected when considering the negative sign associated with in Eqn. (1). Negative sign combined with positive length factor c indicates that the proposed strain gradient model takes less account of strain effect compared with classical Kirchhoff plate model. Although this observation is consistent with theoretic analysis, the difference is so small (10^{-10}) compared with the magnitude of deformation (10^{-3}). We

believe that the reason why the two factors have small effect on overall deformation is because we enforced all zero boundary conditions, similar observations have also been found in [26].

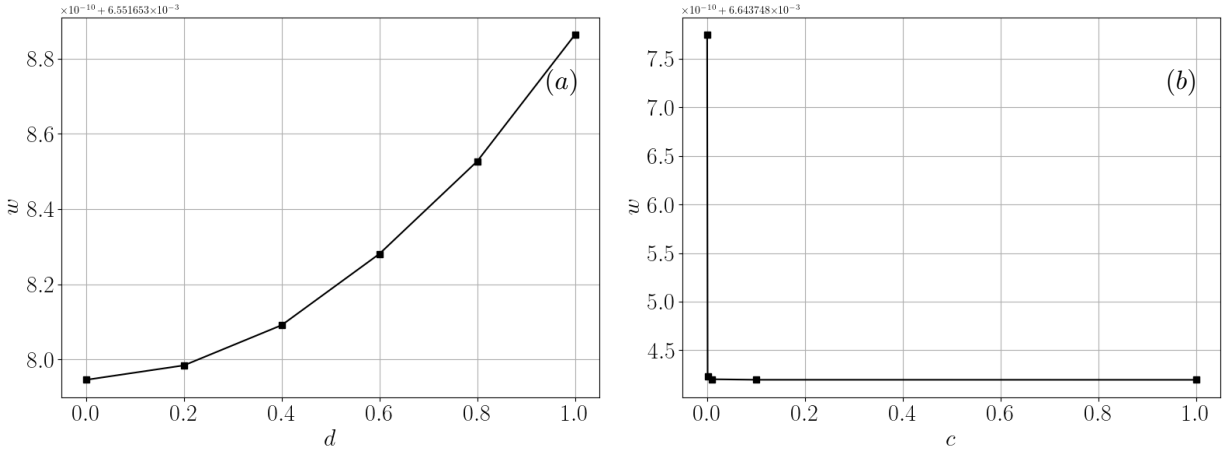

Figure 5: The change of out-of-plane displacement w with respect to (a)the ratio of Von Kármán nonlinearity d and (b)characteristic length factor c. All simulations are performed based on 15×15 mesh.

4.2 Performance analysis

We have also tested finite element algorithm performance by choosing different problem scale $N = [2, 4, 8, 16, 32]$. All the cases are tested on the same machine with processor Intel Core i7-9750H CPU @ 2.60GHz and available memory up to 16GB. Fig. (6) shows the results of benchmark. It is observed that as N increases, both time and memory consumption show quadratic growth.

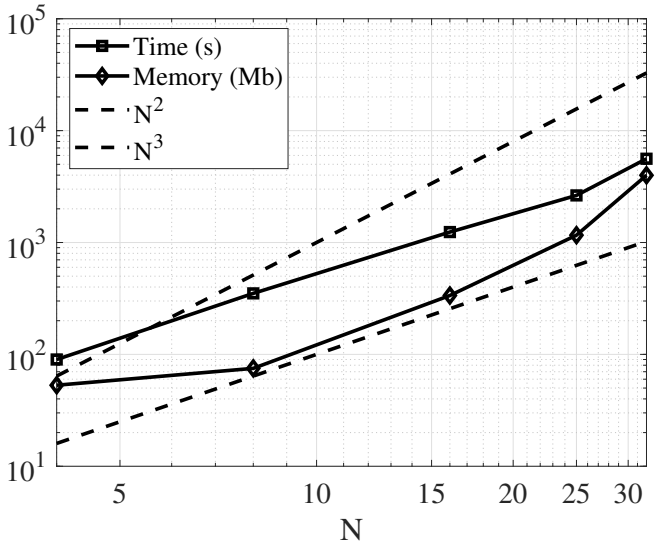

Figure 6: Time and memory consumption with respect to the growth of nodal number. N is number of points on x and y direction. Total number of points and final equations of linear system are N^2 and $(12N)^2$.

For largest problem scale $N = 32$, the total degrees of freedom DOF $= (12N)^2 = 147456$, which is much larger than the true problem scale 1024 if only w is considered as unknown variable for classical Kirchhoff plate theory. Again it should be pointed out that although in this study we use 12 unknown variables for each

node, a convergent finite element scheme can be obtained using C^0 continuity shape function only. Future works will be focused on developing more efficient finite element algorithms for solving such problems.

5 Conclusion

In this work, we have proposed a C^0 continuity finite element formulation along with analytic formulation of von Kármán based nonlinear strain gradient Kirchhoff plate model. The main outcome of this work lies on the systematic derivation of NSGKLPT and finite element formulation. In particular, we developed a novel FEM for solving 4^{th} order PDEs using only C^0 continuity shape function. To do this, we transformed original problem with 3 governing equation and variables into an equivalent problem with 12 governing equation and variables. This transformation enables us to find approximate solutions to satisfy 4^{th} order equations with only C^0 continuity on the whole domain. Numerical simulations indicate that the proposed method show good convergence for under different configurations of nonlinear and strain gradient effect.

Besides of main contribution, it should be mentioned that current study builds on the assumption of all homogeneous boundary conditions derived in weak form formulation, which is not true as it is in classical plate problem (Classical plate problems often involve with boundary conditions such as simply supported and clamped boundary). This assumption has also affect strain gradient behaviour shown in Fig. (5) such that strain gradient has little effect on overall deformation. Combining this observation with computational performance, future works should be focused on developing more efficient FEM by incorporating boundary condition analysis.

Acknowledgements: The following work was supported by course Nonlinear Finite Element Method, ME597 at School of Mechanical Engineering, Purdue University under the guidance of Dr. Adrian Buganza Tepole. The content and information presented in this manuscript do not necessarily reflect the position or the policy of the government. The material is approved for public release; distribution is unlimited.

Author Contributions: All authors have contributed equally to literature survey and manuscript writing.

Competing Interests: The authors declare that there are no competing interests.

References

[1] Singiresu S Rao. Vibration of continuous systems, volume 464. Wiley Online Library, 2007.

[2] Jerome J Connor and Susan Faraji. Fundamentals of structural engineering. Springer, 2016.

[3] Olivier Andre Bauchau and James I Craig. Structural analysis: with applications to aerospace structures, volume 163. Springer Science & Business Media, 2009.

[4] Millard F Beatty. Topics in finite elasticity: hyperelasticity of rubber, elastomers, and biological tissues—with examples. 1987.

[5] Stuart S Antman. Nonlinear plasticity. In Nonlinear Problems of Elasticity, pages 603–628. Springer, 1995.

[6] Tien-Chien Chang and Richard A Wysk. Computer-aided manufacturing. Prentice Hall PTR, 1997.

[7] Morton E Gurtin. An introduction to continuum mechanics. Academic press, 1982.

[8] K Magnucki, M Malinowski, and J Kasprzak. Bending and buckling of a rectangular porous plate. Steel and Composite Structures, 6(4):319–333, 2006.

[9] Maenghyo Cho and R Reid Parmerter. Efficient higher order composite plate theory for general lamination configurations. AIAA journal, 31(7):1299–1306, 1993.

[10] Wu Lanhe. Thermal buckling of a simply supported moderately thick rectangular fgm plate. Composite Structures, 64(2):211–218, 2004.

[11] Danielle L Miller and Tarun Goswami. A review of locking compression plate biomechanics and their advantages as internal fixators in fracture healing. Clinical Biomechanics, 22(10):1049–1062, 2007.

[12] Amir R Askari and Masoud Tahani. Size-dependent dynamic pull-in analysis of beam-type mems under mechanical shock based on the modified couple stress theory. Applied Mathematical Modelling, 39(2):934–946, 2015.

[13] J S Stölken and AG Evans. A microbend test method for measuring the plasticity length scale. Acta Materialia, 46(14):5109–5115, 1998.

[14] David CC Lam, Fan Yang, ACM Chong, Jianxun Wang, and Pin Tong. Experiments and theory in strain gradient elasticity. Journal of the Mechanics and Physics of Solids, 51(8):1477–1508, 2003.

[15] Dennis C Rapaport. The art of molecular dynamics simulation. Cambridge university press, 2004.

[16] Saeid Sahmani, Mohammad Mohammadi Aghdam, and Timon Rabczuk. Nonlocal strain gradient plate model for nonlinear large-amplitude vibrations of functionally graded porous micro/nano-plates reinforced with gpls. Composite Structures, 198:51–62, 2018.

[17] Augustus Edward Hough Love. Xvi. the small free vibrations and deformation of a thin elastic shell. Philosophical Transactions of the Royal Society of London.(A.), (179):491–546, 1888.

[18] Raymond David Mindlin. Second gradient of strain and surface-tension in linear elasticity. International Journal of Solids and Structures, 1(4):417–438, 1965.

[19] Raymond David Mindlin and NN Eshel. On first strain-gradient theories in linear elasticity. International Journal of Solids and Structures, 4(1):109–124, 1968.

[20] Richard A Toupin. Theories of elasticity with couple-stress. 1964.

[21] A Cemal Eringen and DGB Edelen. On nonlocal elasticity. International journal of engineering science, 10(3):233–248, 1972.

[22] Inna M Gitman, Harm Askes, and Elias C Aifantis. The representative volume size in static and dynamic micro-macro transitions. International Journal of Fracture, 135(1-4):L3–L9, 2005.

[23] Jinseok Kim and JN Reddy. A general third-order theory of functionally graded plates with modified couple stress effect and the von kármán nonlinearity: Theory and finite element analysis. Acta Mechanica, 226(9):2973–2998, 2015.

[24] AR Srinivasa and JN Reddy. A model for a constrained, finitely deforming, elastic solid with rotation gradient dependent strain energy, and its specialization to von kármán plates and beams. Journal of the Mechanics and Physics of Solids, 61(3):873–885, 2013.

[25] J Meenen and H Altenbach. A consistent deduction of von kármán-type plate theories from three-dimensional nonlinear continuum mechanics. Acta Mechanica, 147(1-4):1–17, 2001.

[26] Bishweshwar Babu and BP Patel. An improved quadrilateral finite element for nonlinear second-order strain gradient elastic kirchhoff plates. Meccanica, 55(1):139–159, 2020.

[27] Shuo Liu, Tiantang Yu, Tinh Quoc Bui, and Shifeng Xia. Size-dependent analysis of homogeneous and functionally graded microplates using iga and a non-classical kirchhoff plate theory. Composite Structures, 172:34–44, 2017.

[28] M Bacciocchi, N Fantuzzi, and AJM Ferreira. Conforming and nonconforming laminated finite element kirchhoff nanoplates in bending using strain gradient theory. Computers & Structures, 239:106322, 2020.